[1]Yicheng LIU
[2]Fei WANG*
[1]Jiading WANG
[2]Yun LI

Research on Landslide Failure of Rainfall-type Accumulation Body Based on Physical Model

Journal of Electrical Systems

Abstract: - The occurrence of landslides in accumulation bodies is significantly influenced by rainfall, which has been prevalent in southwestern China in recent times. Consequently, investigating the alterations in the internal volumetric water content, pore water pressure, and the migration patterns of fine particles within these bodies under varying rainfall scenarios holds considerable importance. Utilizing a physical model test, researchers delve into the failure mechanisms of the accumulation body under three distinct rainfall conditions, employing a multi-functional integrated sensor embedded within the model to facilitate this analysis. The test results are as follows: Under the rainfall conditions of 30, 50 and 70mm/h, the failure modes of accumulation slope are simple cracking, pull failure after traction and collapse failure respectively. With the gradual increase of rainfall, the response rate of sensors buried in the same location also increases, but the increase of pore water pressure is equivalent to the lag of volume water content. Through quantitative analysis, it is proved that fine particle migration is the direct factor of landslide of loose deposits induced by rainfall. Finally, the mechanism of slope instability and failure induced by different degrees of rainfall is proved, and the relevant results can provide scientific theoretical basis for the early warning of similar slope in southwest China.

Keywords: Rainfall condition; Accumulation; Model test; Multi-functional integrated sensor; Volume moisture content; Pore water pressure; Fine migration

1 INTRODUCTION

Landslides are one of the most common catastrophic geological disasters both domestically and internationally [1]. Relevant statistical data shows that from 2013 to 2023, there were a total of 71,583 landslides in China, accounting for 69.73% of the total number of geological disasters in the country [2]. Surveys indicate that geological disasters in the southwestern regions of Sichuan, Chongqing, and Guizhou are the most frequent, with accumulation body landslides being the most prominent [3]. Accumulation bodies are widely distributed in mountainous areas as a type of poor geological body. They are the product of slope deformation and destruction, and are a set of Quaternary geological bodies with diverse origins, complex components, disordered structures, and mixed soil and stone accumulation [4]. Due to the strong permeability of accumulation bodies, they have poor inherent stability and are extremely susceptible to the impact of rainfall and other hydrological factors, leading to instability and destruction. Data shows that in the Wanzhou District of the Three Gorges Reservoir area, accumulation body landslides accounted for 63% of the total number of landslides in 2023 [5]. Among them, the loss of life and property caused by rainfall-induced accumulation body landslides is the most severe. Therefore, studying the mechanism of destruction of loose accumulation bodies under various rainfall conditions is particularly important.

[1] * Department of Geology/State Key Laboratory of Continental Dynamics, Northwest University, Xi 'an 710127, Shaanxi, China.Email:wf@nwu.edu.cn

[2]China Railway Changjiang Traffic Design Group Co., LTD., Chongqing 401147, China.

At present, the academic community has conducted extensive research on the phenomenon of accumulation body landslides triggered by rainfall, covering various aspects such as field measurement [6-8], numerical simulation [9-11], and model testing [12-14].

In terms of field measurement, Lin Song et al. [15] conducted in-depth understanding of the key factors affecting landslide disasters through comprehensive geological and grid high-density electrical method measurement techniques, providing a scientific basis for the prevention and management of landslide disasters; Zhang Yi et al. [16] conducted on-site double-ring permeability tests on each layer of the accumulation layer landslide in the Duanheba area, and combined with high-density electrical method field detection technology to assess the volume water content of each layer, and found that rainfall-induced accumulation body landslides are due to the existence of permeability coefficient differences within the landslide, thus forming an infiltration channel.

Regarding numerical simulations, Xu Ping and colleagues [17] employed the instability of the accumulation body slope proximate to Majiagou in the Three Gorges Reservoir region as a case study. They constructed a corresponding numerical analysis model to assess the impact of the reservoir's water level fluctuations within a single hydrological cycle on the slope's safety factor, utilizing the strength reduction method. Meanwhile, MENM and their team [18] investigated the underlying mechanism of the accumulation body slope's response to rainfall infiltration, drawing from a comprehensive review of actual engineering data. They derived infiltration rate formulas for the slope both before and after water accumulation, and subsequently employed numerical software to quantify the slope's stability. This analysis illuminated the patterns of stability variation exhibited by soil slopes under rainfall infiltration conditions.

In terms of model testing, Chen Yulong et al. [19] took the accumulation body landslide as the research object, and through large-scale model tests under rainfall conditions, explored the seepage, deformation, and destruction rules of the accumulation body slope, and studied the feasibility of acoustic emission as an early warning criterion. Liu Cheng et al. [20] explored the movement and accumulation characteristics of landslide-debris flow under different slope degrees and widths through indoor small-scale model tests, and finally found that an increase in slope degree would lead to an increase in the travel distance and coverage area of fine-grained accumulation bodies, thereby making the degree of landslide destruction more severe.

In summary, rainfall-induced accumulation body landslides are a complex process affected by various factors. In order to deeply understand this phenomenon, predecessors have carried out a lot of work from different angles. These studies not only involve the structural composition of the accumulation body but also include mechanical property tests, revealing the impact of different intensities of rainfall on the mechanical properties of the accumulation body. Based on these research results, this experiment will construct physical models of accumulation bodies under different rainfall intensities and carry out various working conditions of finite element analysis to provide feasibility basis for the model. Finally, by embedding sensors to monitor the internal mechanical changes of the accumulation body, explore the law of the change of the destruction mode of the accumulation body with the change of rainfall intensity. This experiment will deepen our understanding of the development characteristics of accumulation body landslides under different rainfall intensities, and provide a solid scientific basis for early warning analysis of landslides in extreme rainfall conditions. Through precise data analysis and theoretical models, we can more accurately predict the risk of landslides, formulate effective prevention measures, to protect the safety of people's lives and property.

2 MODEL TEST OF ACCUMULATIVE RAINFALL LANDSLIDE

The physical model can describe qualitatively or quantitatively the change of slope body under the action of external force from a macroscopic point of view, and can reveal the change of physical quantity of rock and soil body during the failure process. In this paper, based on a landslide in Wanzhou District of Chongqing City, a physical model test of landslide rainfall is conducted to simulate the whole process of instability failure of a landslide slope with the same rock content after three different degrees of heavy rainfall. In this process, the corresponding law of the variation of various physical quantities of the accumulation slope and the vertical migration law of soil particles under different rainfall intensity are analyzed.

2.1 Test scheme

2.1.1Model parameter setting

According to relevant studies, landslide disaster is closely related to the rainfall intensity of the day: If the rainfall intensity of the day reaches the rainstorm level, that is, the rainfall reaches 50~90mm, the probability of landslide of the accumulation body is close to 92%[21]. Therefore, this paper establishes three distinct rainfall intensity levels, specifically 30mm/h, 50mm/h, and 70mm/h, with the goal of comprehensively simulating cumulative landslides induced by varying rainfall intensities. In the majority of physical model experiments, the similarity ratios among the physical quantities within the model are primarily influenced by the geometric shape of the slope [22]. Upon the determination of the slope's geometric characteristics, the corresponding similarity ratios for other physical quantities can be derived [23]. Based on the height of the prototype slope and the unique soil properties of the sampling area, an appropriate similarity scale can be established for the model to mimic the conditions of the prototype slope under specific scenarios. Therefore, the geometric scale factor λ can be preliminarily set as 100 based on the model tank's size. Dynamic similarity relations between the model and prototype are derived through applying gravity similarity laws and dimensional analysis methods in landslide model testing [24-25]. Detailed similarity relationships are shown in **Table 1**.

Table 1 Ratios of model scale

Physical parameter	Similar relationship	Similar ratio
Geometric dimension（l）	C_l	100
Soil density（ρ）	C_ρ	1
Cohesive force（C）	$C_C = C_\rho * C_l$	100
Angle of internal friction（φ）	C_φ	1

Therefore, the overall height of the model is controlled at 50cm, the width is controlled at 60cm, and the length is controlled at 90cm. Chen[26] studied the accumulation body in the Three Gorges area and found that landslide was most likely to occur when the slope foot of the accumulation body developed to 20°~40°. However, considering that the safety factor of real landslide was generally smaller than that of the model, the model slope

foot was set at 50°. Moreover, it is acknowledged that the overall stability improves with an increase in the deposit body's dry density. Thus, in this model test, the dry density of the test soil sample is specified at 1.5g/cm3, the water content is maintained at 7%, and the stone content within the deposit body is set to 30%. Detailed soil sample parameters are shown in **Table 2**.

Table 2 Model test plan

Working condition	Rainfall intensity/mm·h^{-1}	Stone content of deposit body/%	Slope Angle/°	Dry density/g·cm^{-3}	Moisture content/%
G1	30				
G2	50	30	50	1.5	7
G3	70				

The model test soil sample was selected from the landslide area less than 3cm gravel soil. After measurement and calculation, the mass percentage of particles larger than 2mm in the soil sample used for test is 72.2%, the effective particle size is d_{10}=0.5mm, the continuous particle size is d_{30}=2.3mm, the control particle size is d_{60}=4.2mm, 10 < C_u=12, 1 < C_c=2.37 < 5, and the soil particle distribution is shown in **Fig.1**.

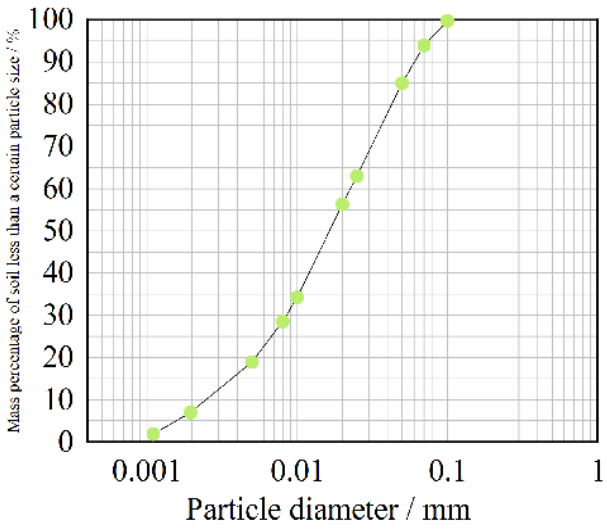

Fig.1 Particle gradation curves of accumulation

2.1.2 Check the test parameters

Based on the setting of various parameters of the physical model and the soil physical parameters obtained in the indoor experiment, as shown in **Table 3**, the stability of the accumulation body Slope with a slope foot of 50° was checked by the Slope/w plug-in of the numerical simulation software Geostudio based on the limit equilibrium method, so as to ensure the stability of the accumulation body model under natural conditions. Then the Mohr-Coulomb criterion, which is the most widely used at present, was further adopted [27], namely:

$$\tau = c' + (\sigma - u_a)\tan\varphi' + (u_a - u_w)\tan\varphi^b \quad (1)$$

Where: τ is the shear strength of unsaturated soil; σ is the total normal stress; u_a and u_w are pore gas pressure and pore water pressure, respectively. The stability of accumulative body under three different conditions of rainfall intensity is analyzed, and the setting of rainfall intensity conditions in the model test meets the conditions of precipitation induced landslide of accumulative body. The specific simulation results are shown in **Fig.2**.

Table 3 The values of soil mechanical parameters are adopted

Stratum	Natural weight/kN·m^{-3}	Friction Angle in rock and soilφ/°	Cohesion of rock and soil mass$C$/kPa	Bearing capacity characteristic value/kPa
Boulder soil	22.0	32	53	1000

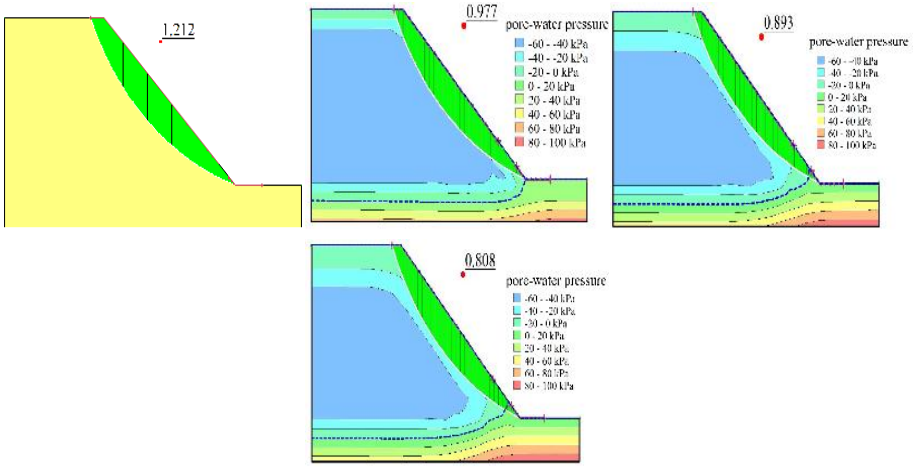

（a）Natural condition （b）G1 condition （c）G2 condition （d）G3 condition

Fig.2 Numerical simulation results of accumulation model under different working conditions

2.1.3 Accumulation body model preparation

The preparation process of the model consists of the following six steps: sieve mixing, outline, layered construction, buried instrument, adjustment of slope shape, and static observation. The steps are described as follows:

(1) screening and mixing: use a 1cm filter screen to separate the soil and gravel, and put them in two areas for reserve. Then the fixed volume of soil and gravel is mixed according to the set dry density, moisture content and gravel content of the soil sample.

(2) Outline the outline: mark the slope Angle with tape on the glass on both sides of the landslide model groove, which is convenient for later model specification production.

(3) Layered construction: Pour the mixed soil into the model tank evenly in batches, and compacted the soil after each pouring to enhance the stability of the soil in the natural state. And in order to prevent the boundary phenomenon of each layer, it is necessary to plane the surface of each layer to form a complete accumulation body.

(4) Buried instrument: In order to prevent the buried sensor from affecting the model, the sensor should be buried in the layered construction process, and the buried position of the same type of sensor should be 10cm apart.

(5) Slope shape adjustment: After the entire slope is built, the slope should be flattened by reference to the contour line to facilitate subsequent observation of the model.

(6) Static observation: After the slope is built, it needs to be static for 1 hour, and the overall stability can be judged according to the message returned by the data acquisition instrument. The rainfall test can be started after the data is stable.

Three cameras were arranged at the site to observe and record the damage and deformation of the slope in the process of rainfall in real time. The three cameras were located directly in front of the slope, directly above the slope and on the right side of the slope. The test starts with the rainfall device being started and ends with the slope not having sustained failure.

2.2 Test apparatus

This physical test was carried out in the landslide physical model tank, and the physical model test device mainly consisted of three parts: artificial simulated rainfall system, debris flow landslide simulation tank, and multi-functional integrated sensing system. The specific model device size is shown in **Fig.3**. It is worth mentioning that the multifunctional integrated sensor used in the test needs to be calibrated to the receiving software before the test, through the formula:

$$K = \frac{\rho g h}{V_1 - V_0} \tag{2}$$

Where,K is the calibration coefficient,ρ Is the density of water,g is the acceleration of gravity,h is the depth of sensor embedment,V_1 is the buried voltage,V_0 is the initial voltage.

A combined artificial rainfall device was used in the experiment, and the main body was composed of shower plate and electromagnetic pump. In order to ensure uniform rainfall in the test area, the spacing of rain nozzles is designed to be 5cm, and the number of nozzles is 50. The electromagnetic pump and pressure valve facilitate the adjustment and calibration of rainfall, enabling it to attain the predetermined rainfall intensity for three distinct operational scenarios. Subsequent to the installation of the mounting apparatus, a rain gauge is strategically positioned at the corner of the water tank during precipitation, allowing for real-time monitoring of rainfall intensity to ensure adherence to the specified operational conditions.

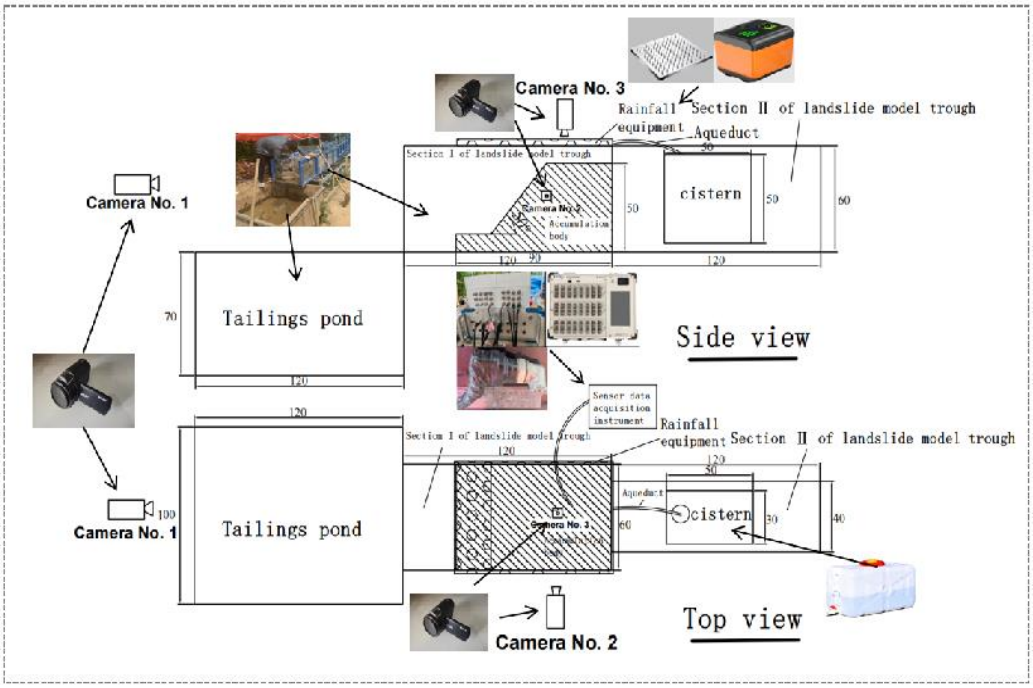

Fig.3 Physical model device size drawing (unit: cm）

3 ANALYSIS OF TEST RESULTS

3.1 Failure process analysis of accumulation body model

Three rainfall intensities were set in this model test: 30mm/h, 50mm/h and 70mm/h. As the rainfall continues, the accumulation body model changes as follows.

(1) In the test of rainfall intensity of 30mm/h (**Fig.4a**), because the rainfall intensity did not reach the rainstorm level, a slight transverse crack appeared at the foot of the accumulation body until the rainfall lasted for 29min, and there was no significant change at the top of the slope. As rainfall persisted for 58 minutes, cracks at the slope's base developed and widened, triggering slight liquefaction in the slope's center. After 98 minutes of rainfall, longitudinal cracks emerged on the slope's side, transverse cracks widened at the base, and significant displacement occurred, though no sliding was observed.

(2) In the test of rainfall intensity of 50mm/h (**Fig.4b**), local sliding occurred at the bottom of the accumulation body when the rainfall lasted 22min. Moreover, cracks in other non-slip regions of the accumulation body remained unchanged in number and width. By 47 minutes, the erosion zone extended upwards to the slope's midpoint, with no sign of overall sliding in the local slope area throughout the process. Finally, when the rainfall reached 89min, the left side of the accumulation body began to liquefy in a large area, the right side cracks appeared, and the slope foot of the accumulation body collapsed.

(3) In the test of rainfall intensity of 70mm/h (**Fig.4c**), when the rainfall lasted for 16min, gullies appeared at the slope foot of the accumulation body. As the rainfall persisted for 37 minutes, the gully underwent intensified erosion and expansion due to rainwater's impact, while cracks emerged in the central region of the slope's base. These gullies and cracks facilitated further erosion of the slope's crest by rainwater. After 81 minutes of the test, minor collapse was observed on the crest of the accumulation body. Post-rainfall, numerous cracks and collapses were evident across the entire slope. Continuous rainfall would expedite rainwater infiltration and accelerate slope

deformation.

T=29min *T*=58min *T*=98min

（a）30mm/h

T=22min *T*=47min *T*=89min

（b）50mm/h

T=16min *T*=37min *T*=81min

（c）70mm/h

Fig.4 Deformation and failure process of landslide model under three rainfall intensities

3.2 Change of volumetric water content and pore water pressure

The multi-functional integrated monitoring apparatus is capable of real-time surveillance of water content and pore water pressure variations within the accumulation body. For this purpose, three PR25-CH1 pore water pressure sensors and three MTD05 moisture sensors were employed to continuously track changes in volumetric water content within the slope. The sensors operate at a frequency of 1000HZ, and data is recorded every minute, considered valid for analysis.

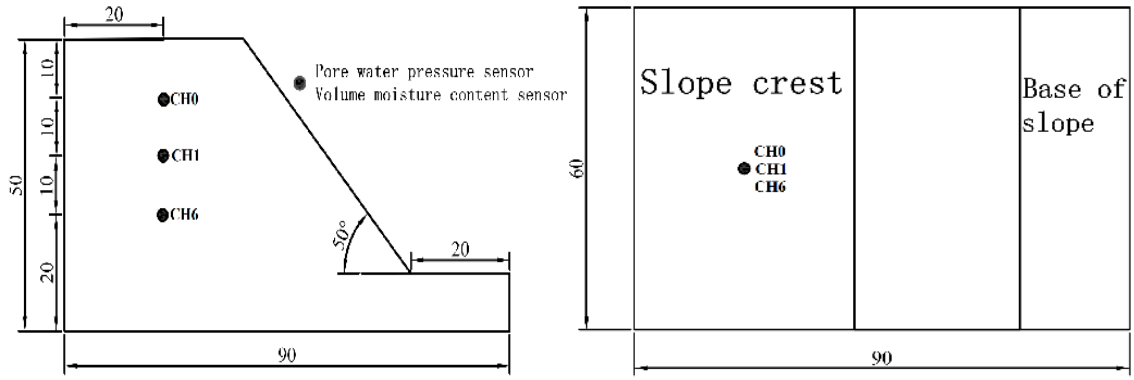

（a）Side view　　（b）Top view

Fig.5 Layout of sensors (unit: cm)

3.2.1 Volumetric water content change

(1) **Fig.6a** illustrates the data recorded by the volumetric moisture content sensors during a rainfall intensity of 30mm/h. The maximum volumetric water content measured by sensors CH0, CH1, and CH6 is 26.2%, 29.9%, and 34.8% respectively, exhibiting a trend that aligns with the variation pattern observed in pore water pressure. Although pore water pressure and volume water content change in the same trend during rainfall, at any time, the former lags behind the latter. This indicates that pore water pressure increases sharply only after soil saturation.

(2) The data displayed by the volumetric moisture content sensor at a rainfall intensity of 50mm/h are shown in **Fig.6b**. As can be seen from the figure, the change of overall water content can be divided into initial stable stage, rapid increase stage and stable stage. Considering that the three sensors are buried in different depths inside the accumulation body, taking the CH1 sensor as an example, the value of CH1 began to rise at 22 minutes with the progress of rainfall. Then the soil began to saturated, and the volume water content reached a stable state of 27%, and the whole began to stabilize.

(3) The data displayed by the volumetric moisture content sensor at a rainfall intensity of 70mm/h are shown in **Fig.6c**. The change of the volume water content from the top to the bottom of the slope in the vertical direction also reflects the mutual flow process between the slopes. Based on the separation distance (10cm) between the sensors and the increase in rainfall time, the infiltration ratio can be calculated. The permeability of the three sensor layers is 2.78×10^{-4}m/s, 1.33×10^{-4}m/s and 1.34×10^{-4}m/s, respectively, which is approximately equal to the soil permeability measured before the test. The different time required to reach the same value also indirectly reflects the hydrologic process of cross-flow along the slope. However, water preferentially accumulates from the top to the bottom, resulting in a larger peak volume water content measured in CH6 than in other locations.

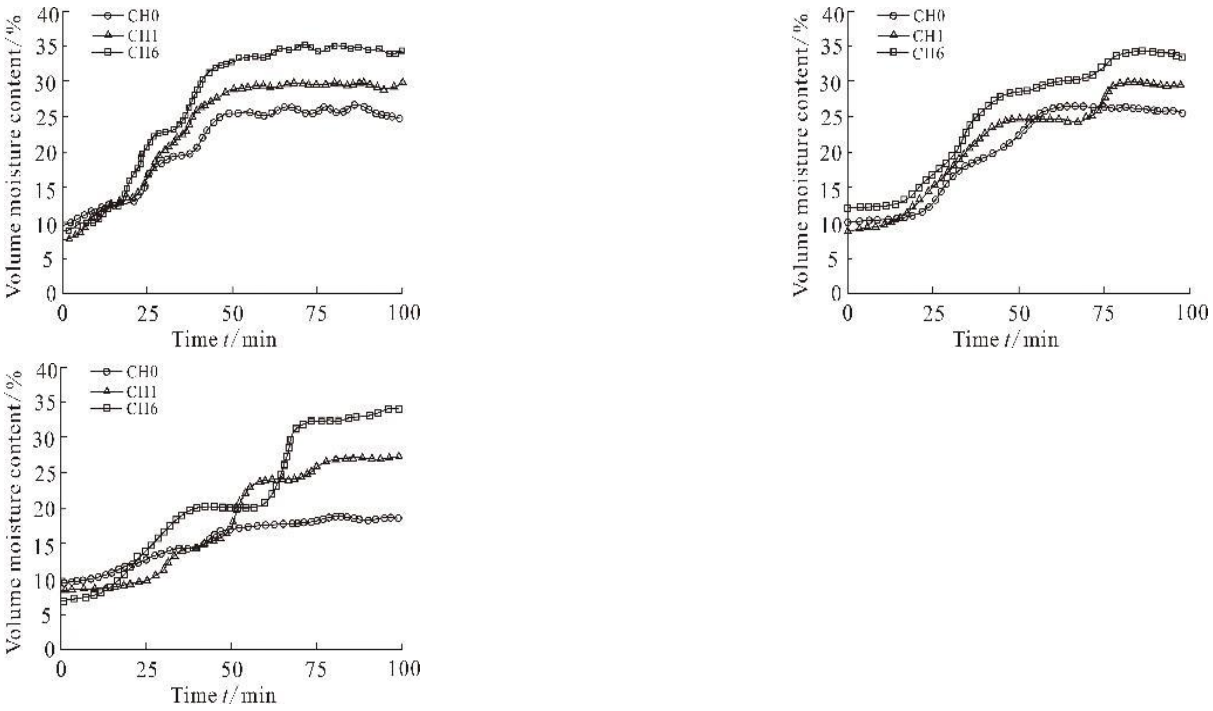

（a）Rainfall intensity 30mm/h （b）Rainfall intensity 50mm/h （c）Rainfall intensity 70mm/h

Fig.6 Volume moisture content curve of slope under different rainfall intensity

3.2.2 Pore water pressure changes

Pore pressure encompasses the pressure exerted by both pore fluids—water and gas—within soil. Comprehending the dynamics and distribution of pore water pressure is instrumental in assessing the stability and engineering security of loess, while also enhancing understanding of groundwater movement and soil mechanical characteristics [28]. An analysis of the three pore water pressure measurement points located on the slope yielded the following findings:

(1) As depicted in **Fig.7a**, the pore water pressure sensor recorded data during a rainfall intensity of 30mm/h. When plotting the variation of pore water pressure against rainfall duration, the maximum dynamic pore water pressure within each loading period is taken into account. Specifically, the CH0 sensor, positioned near the slope's base of the accumulation body, registers a gradual increase in pore water pressure with the elongation of rainfall duration, culminating in a peak value of 0.5453kPa after 28 minutes of rainfall. There was no abnormal fluctuation after reaching the peak until the end of the test. This indicates that the surface deposit has begun to liquefy to a certain extent, which is corresponding to the change of water content mentioned above.

(2) The display data of the pore water pressure sensor under the rainfall intensity of 50mm/h is shown in **Fig.7b**. At the beginning of the experiment, with the increase of rainfall, the CH1 value of the monitoring point has a tendency to increase rapidly, which is due to the rapid seepage speed of the measuring point. Thereafter, the seepage rate slowed down and the growth rate of pore water pressure began to slow down after the rainfall lasted for 37min. In the cracking stage of the accumulation body, the gap between the soils increases, and the CH1 sensor quickly reaches a peak value of 1.0458kPa.

(3)**Fig.7c** presents the pore water pressure sensor's readings during a rainfall intensity of 70mm/h. In comparison to the previous two rainfall intensities, the CH6 sensor's response rate notably escalated under the 70mm/h scenario, achieving a peak value of 1.7256kPa within 83 minutes. This underscores that, with all other external factors being equal, the infiltration rate of the accumulation slope intensifies as rainfall intensity increases. After attaining their respective maximum values, all three sensors exhibit slight fluctuations, suggesting that the loss of fine particles within the slope also exerts an influence on the sensors' readings.

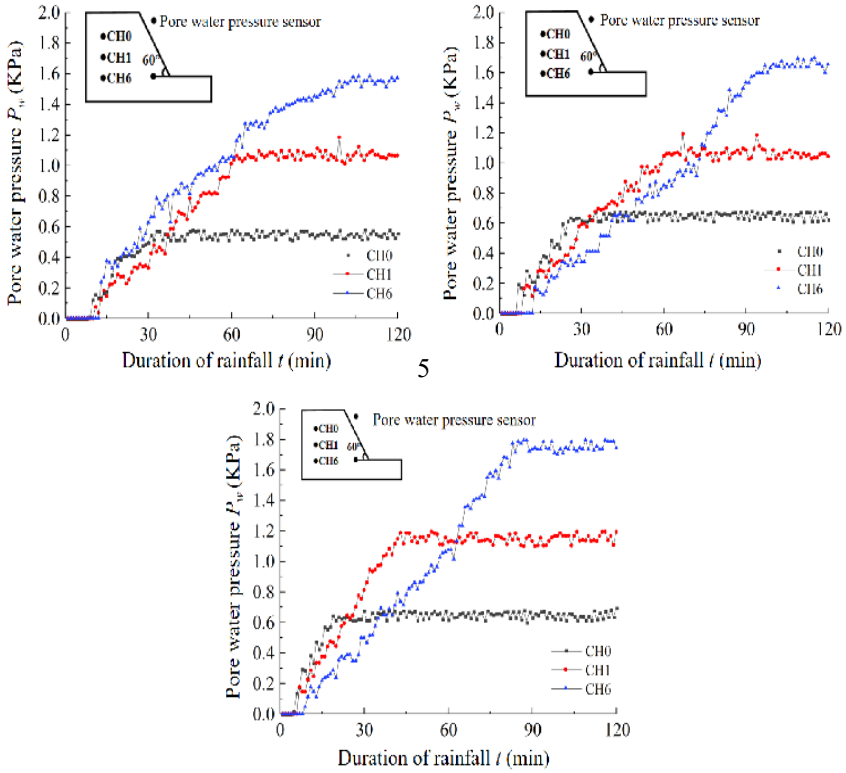

（a）Rainfall intensity 30mm/h　　（b）Rainfall intensity 50mm/h　　（c）Rainfall intensity 70mm/h

Fig.7 Pore water pressure curve of slope under different rainfall intensity

3.3 Fine particle migration during landslide

With the continuous rainfall, the finer particles inside the accumulation body will be carried by the rain and left along the slope. Under various rainfall intensities, the migration rates of fine particles exhibit differences. Based on three different rainfall scenarios, this study also conducts an in-depth discussion on the loss rate of fine particles. Given the difficulty of directly observing the fine particle content in the accumulation body with the naked eye, the experiment adopts the method of sampling survey, aiming to scientifically analyze the migration law of fine particles in the accumulation body. Specific test methods are as follows: For the three groups of tests, samples were taken from the top of the slope along the slope every 15cm at the same position on the slope, and the sampling quality was 300g; The soil sample is mixed with 300g water in equal proportion to form a suspension. After configuration, the three groups of samples were passed through 0.1mm fine sieve respectively, and dried to count the final quality; The grain gradation curves of the accumulation body after three different intensities of rainfall are drawn. The final results are analyzed as follows:

(1) Under G1 condition, the fine particle content at each position inside the accumulation body is shown in **Fig.8a**. From the graph, it can be interpreted that when the rainfall intensity does not reach the level of heavy rain, the content of fine particles at the top of the slope changes little before and after the rainfall, with only a difference of 0.3%. However, compared with the initial state, the decrease in the content of fine particles at the bottom of the slope is also relatively small, only 0.46%. **Fig.9a** shows the detailed situation of fine particles at the slope toe. It is noteworthy that the content of fine particles at the bottom of the slope is significantly higher than that at the top and middle, suggesting that during the migration process, fine particles tend to accumulate from the top and middle of the slope to the bottom. Further observation of Figure 9a reveals that the sediment structure at the slope toe is not uniform but exhibits distinct layering characteristics, with clay at the bottom and fine gravel covering it. This phenomenon indicates that the initial stage of accumulation deformation is often accompanied by the migration of fine particles. As a large number of fine particles migrate, their original supporting role weakens, leading to the loosening of large particles and ultimately potentially causing a landslide in the accumulation.

(2) Under the G2 setting conditions, the distribution of fine particles in various regions of the accumulation body is shown in **Fig.8b**. Compared with the G1 conditions, the rainfall intensity of G2 has reached the level of a heavy rainstorm. At this time, the content of fine particles in the top and middle regions of the slope both decreased significantly, specifically, the top decreased to 7.40%, and the middle decreased to 8.10%. Although the content of fine particles at the bottom of the slope remains relatively high at 9.23%, according to the depiction in **Fig.9b**, the content of fine particles at the slope angle of the accumulation body has increased significantly. This indicates that although most of the fine particles from the top and middle of the slope will eventually erode and accumulate at the bottom of the slope, considering the increase in fine particles at the slope angle, the actual net loss rate of fine particles at the bottom of the slope is expected to exceed 0.77%.

(3) Under G3 working condition, the fine particle content at each position inside the accumulation body is shown in Figure **Fig.8c**. Under the G3 scenario, the rainfall intensity rose to 70mm/h, far exceeding the definition standard of a heavy rainstorm, leading to the most significant loss of fine particulate matter. Specifically, the content of fine particles in the top of the slope decreased to 6.77%, further decreasing to 6.21% in the middle of the slope, while the bottom of the slope remained at 8.50%. It is worth noting that as the rainfall intensity continues to climb, the loss rate of fine particulate matter also accelerates. Before the rainwater begins to infiltrate the soil, runoff will first form on the slope surface, which results in a relatively smaller loss of fine particulate matter in the top of the slope compared to the middle of the slope.

(4) As can be seen from **Fig.10**, there are obvious differences in particle gradation under the three working conditions. These differences can potentially be attributed to two factors: sedimentary history and the migration of fine particles post-deposition, triggered by rainfall. Rainwater brings particles into the soil through the macropores, and the physicochemical interaction of water (erosion, dissolution, hydrolysis, etc.) changes the strength of cementation between particles, resulting in the separation of particles inside the accumulation body. These fine particles are redistributed and redeposited at certain locations in the soil according to the movement of water.

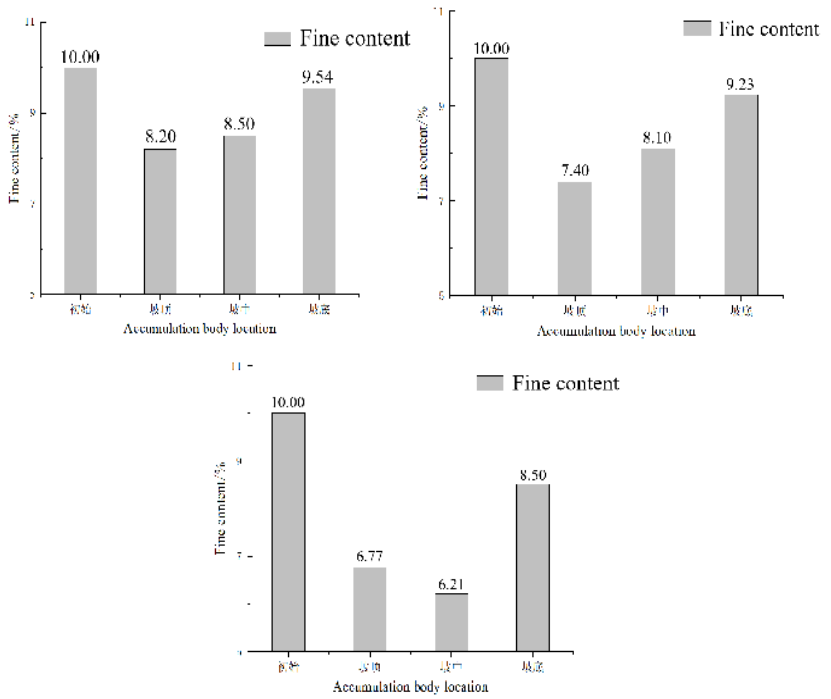

（a）G1 condition （b）G2 condition （c）G3 condition

Fig.8 Fine particle content in each part of accumulation with different rainfall intensity

（a）G1 condition （b）G2 condition （c）G3 condition

Fig.9 Fines content picture at different positions of slopes with different rainfall intensity

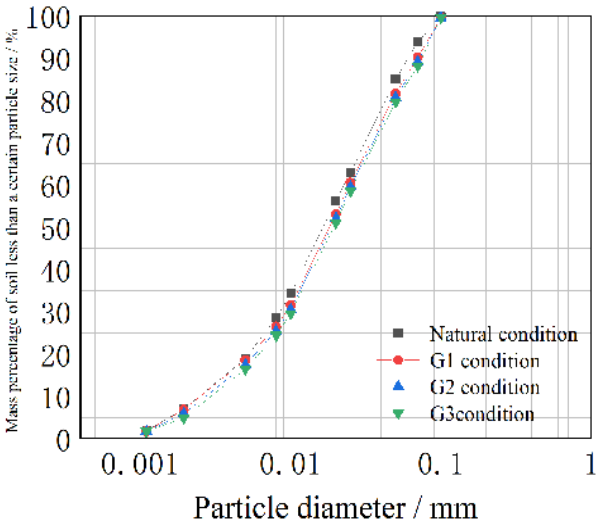

Fig.10 Particle gradation curves of accumulation under different rainfall intensities

4 DISCUSSION

(1) This paper is not based on similar model tests of real slopes, but mainly focuses on the research of landslide hazards such as rain-induced accumulation landslides, which are more typical in southwest China. Therefore, the setting of model test has been simplified, which is similar to the model making method in midweek [29], hoping to reflect a certain type of accumulation through a single model. According to the experimental results of this model, under the rainfall intensity of 30, 50 and 70mm/h, the initial failure of the model is all at the slope Angle. According to the research results of Li Rongjian et al. [30], it may be due to the local three-dimensional effect in the landslide model trough, and the lateral boundary constraints of the model trough will make the test results different from the real situation.

(2) In the course of the test, it can be observed that the total rainfall continues to increase over time although the rainfall intensity is 30, 50 and 70mm/h. However, the critical rainfall for landslide failure is 26.3, 15.2 and 15.8mm, respectively, which indicates that the critical rainfall value for landslide failure does not linearly decrease with the increase of rainfall intensity. This phenomenon is consistent with the results observed by Yang Zongji et al. [31] through Brooks-Corey(BC) and VanGenuchten(VG) models. According to Horton[32] 's slope infiltration theory, we know that the rate of rainfall infiltration is usually much lower than that of slope runoff. During the experiment, rainfall intensity of 70mm/h caused rainwater to swiftly form runoff on the slope surface, before it could penetrate, gradually eroding the slope and ultimately leading to a decrease in slope strength and the generation of turbidity. Conversely, at a rainfall intensity of 50mm/h, the rainwater had ample time to fully infiltrate, boosting soil moisture content and thereby increasing the dead weight. This shift in stress state within the slope body eventually reached a critical point, triggering a landslide. These findings highlight the complex relationship between rainfall intensity and deposit failure, as well as the significant influence of infiltration processes on slope stability.

(3) The current experimental results are inconsistent with the phenomenon described by Cui[33] and Zhou Xiaojun [34] that fine particles form a relatively impervious layer at the foot of slope. In their model test, it was observed that the fine particle content at the foot of slope increased significantly after rainfall, with an increase of 7.8% to 30.12%, which was significantly different from the measured change of fine particle content in this experiment (3.7% to 8.6%). The reason for this difference may be due to the migration, accumulation or blockage of fine

particles that may occur in the process of seepage subsurface erosion. In this experiment, the main observation is particle migration, which increases the soil porosity and accelerates the infiltration of rainwater. Secondly, it may be related to the difference in rainfall intensity and cumulative rainfall. In the flume test of Lei[35] et al., the rainfall intensity was as high as 291.72mm/hour, and the total rainfall was 243.1mm, while the maximum cumulative rainfall in this test model was 108.2mm, showing a big difference. But it also shows a linear relationship between rainfall and the degree of fine particle migration. These factors affect the experimental results, which makes the migration of fine particles in this experiment different from the observed results in previous studies.

5 CONCLUSION

In this paper, a loose accumulation slope in southwest China is taken as the simulation object, and the loose accumulation soil sample is used in the field for outdoor physical model test. Using physical model testing, numerical simulation, and sensor monitoring techniques, researchers have conducted a thorough investigation into the instability and failure mechanisms of loose accumulation slopes under three rainfall rates of 30mm/h, 50mm/h, and 70mm/h. This study focuses on the impact of different rainfall intensities on the physical and mechanical properties of accumulations, and comprehensively analyzes the dynamic changes and response patterns of key physical quantities such as the volumetric water content, pore water pressure, and fine particle content of accumulation slopes under these rainfall conditions.

(1) The difference of rainfall intensity will also change the failure mode of accumulative landslide. When the rainfall intensity has not reached 50mm/h, the main failure mode of landslide is still multi-stage pull-apart. However, when the rainfall intensity gradually increases to 70mm/h, the rainwater will be transformed into surface runoff running down the slope due to insufficient infiltration, and eventually evolve into a collapsive damage mode similar to debris flow.

(2) In the process of model test, the closer the burial position is to the top of the slope, the faster the numerical response of the sensor will be. It shows that the infiltration of rainwater is carried out in the vertical direction, which corresponds to the failure of the landslide surface. In addition, the lagged response of pore water pressure value changes relative to volumetric water content variations underscores the delayed nature of pore water pressure changes during the progression towards landslide failure.

(3) The results of the model experiments reveal that the migration of fine particles in accumulation slopes during rainfall is inevitable, and the degree of their loss is closely related to the intensity of rainfall. Specifically, when the rainfall intensity is 30mm/h, the loss of fine particles is minimal, and the degree of landslide damage is also the least severe. However, as the rainfall intensity increases to 70mm/h, the loss of fine particles becomes most significant, and the degree of landslide damage is also the most severe. It is said that granular migration may be the direct factor of precipitation induced landslide.

REFERENCE

[1] Xiang Zilin. Reliability analysis and risk assessment of landslides in Three Gorges Reservoir area based on odo rless transformation [D]. China Three Gorges University, 2021. (in Chinese)

[2] Wang Bin, LI Jietao, WANG Jiajun et al. Model test of landslide induced by heavy rainfall [J]. Rock and Soil Mechanics, 2023, 44 (S1): 234-248. (in Chinese)

[3] Wang Zigao, Huang Runqiu et al. Research and practice of engineering geology of large deposits in deep valle y in Southwest China [M]. Beijing: China Water Resources and Hydropower Press, 2017. (in Chinese)

[4] LI Yun. Stability analysis and treatment of Mountain road landslide [J]. Transportation Manager World, 2021, (08): 25-26. (in Chinese)

[5] Deng Lizheng, Yuan Hongyong, Zhang Mingzhi et al. Research progress of landslide deformation monitoring a nd warning technology [J]. Journal of Tsinghua University (Science and Technology), 2023, 63(06) : 849-864. (in Chinese)

[6] ZENIL, PICARELLIL, AVOLIOB,et al. Brillouin optical time-domain analysis for Geo technical monitoring[J]. Journal of Rock Mechanics and Geo technical Engineering, 2015, 7(4): 458-462.

[7] Zhang Luming, ZHENG Mingxin, HE Min. Study on matrix suction characteristics of sliding zone soil before and after landslide control [J]. Rock and Soil Mechanics, 2010, 31(10): 3305−3312. (in Chinese)

[8] Deng Lizheng, Yuan Hongyong, Zhang Mingzhi et al. Research progress of landslide deformation monitoring a nd warning technology [J]. Journal of Tsinghua University (Science and Technology), 2023, 63(06): 849-864. (in Chinese)

[9] Guo Jun, Zeng Chao, Xie Mingyu et al. Landslide formation mechanism and accumulation body stability analy sis in Madling Landslide, Guizhou Province [J]. Safety and Environmental Engineering, 2018, 25(02): 48-54+6 0. (in Chinese)

[10] HILLEY G E, BURGMANN R, FERRETTI A. Dynamics of slow-moving landslides from permanent scatter a nalysis[J]. Science, 2004, 304(5679): 1952-1955. (in Chinese)

[11] Xu Chi, JIAN Wenxing, Mei Xinyu et al. Numerical simulation of seepage stress coupling under the combine d action of water level and rainfall in landslide reservoir of Loess Slope in the Three Gorges Reservoir area [J]. Safety and Environmental Engineering, 2017, 24(3): 20-26. (in Chinese)

[12] Hurst index of landslide displacement fractal parameter and its application in landslide prediction of accumulat ion layer [J]. Chinese Journal of Rock Mechanics and Engineering, 2009, 28(06): 1107-1115. (in Chinese)

[13]Li Xiaoen, Zhou Liang, SU Fen-zhen et al. Research progress of InSAR technology in slope disasters [J]. Jour nal of Remote Sensing, 2021, 25(02): 614-629. (in Chinese)

[14] Zuo Zibo, ZHANG Lulu, WANG Jianhua. Model test study of landslides triggered by rainfall of disgraded ac cumulation bodies [J]. Chinese Journal of Geotechnical Engineering, 2015, 37(07): 1319-1327. (in Chinese)

[15] Lin Song, Wang Wei, Deng Xiaohu, et al. Geophysical survey of typical landslides in t-he Three Gorges Rese rvoir area and its significance: a case study of Siangbi landslide in Wanzhou District [J]. Earth Science, 201 9, 44(09): 3135-3146. (in Chinese)

[16] Zhang Yi, Qiao Liang, Zeng Runqiang, et al. Landslide infiltration law of accumulation layer based on in-situ double-ring water seepage test [J]. Journal of Lanzhou University (Natural Science Edition), 2014, 50(05): 666 -670. (in Chinese)

[17] Xu Ping, LI Tonglu, Li Ping. Study on the stability of landslide on the bank of Three Gorges reservoir under unsaturated seepage [J]. Chinese Journal of Geological Hazards and Control, 2010, 21(01): 7-12. (in Chinese)

[18] MEIN R G, LARSON C L. Modeling Infiltration o-n during a steady rain[J]. Water Resources Research, 197 3, 9(2): 384−394. (in Chinese))

[19] Chen Yulong, Huang Dong. Large-scale model test of rain-type accumulation landslide [J]. Journal of Northeas tern University (Natural Science Edition), 2017, 38(04): 576-580. (in Chinese)

[20] Lei Xian-Shun, Zhu Dayong, Liu Cheng, et al. Experimental study on landslide model considering slope and

width of slide [J]. Rock and Soil Mechanics, 2017, 38(5): 1281-1288. (in Chinese)

[21] Qiao Juan, Zhang Liren, Ruan Xiangming. Experimental study on rainfall runoff production and infiltration of landslide soils in Three Gorges Reservoir area [J]. Chinese Journal of Water Resources and Architectural Engi neering, 2013, 11(05): 183-188+193. (in Chinese)

[22] Sedov LI, Friedman M, Holt M, Cole JD. Similarity and dimensional methods in mechanics[J].Appl Mech, 19 61, 28: 159–60. (in Chinese)

[23] Shi Y, Ye Y, Hu N, Huang X, Wang X. Experiments on material proportions for similar materials with high similarity ratio and low strength in multilayer shale deposits[J]. Appl Sci, 2021, 11:9620.

[24] Wujian Y, Xinxin T, Zhijian W, Ping W, Lin K. Seismic effects of loess slopes using physical modeling and numerical simulation[J]. Front Earth Sci, 2023, 10:1058701.

[25] Sun P, Sun H, Lin F, Yang X, Jiang W, Wu W, et al. Experimental study on the ratio model of similar mate rials in the simulation test of coal and gas outburst[J]. Sci Rep, 2021, 11:13513.

[26] CHEN N S, ZHOU W, YANG C L, et al. The processes and mechanism of failure and debris flow initiation for gravel soil with different clay content[J]. Geomorphology, 2010, 121(3-4): 222-230.

[27] Fredlund D.G.hardjo H. Soil mechanics of unsaturated soils [M]. Translated by Chen Zhongyi, Zhang Zaiming, Chen Yujiong et al. Beijing: China Architecture and Construction Press, 1997. (in Chinese)

[28] Zhang X, Pei X, Zhang Z, Song L.Study on pore pressure and fluidization evaluation method of unsaturated l oess in vibration process[J]. Bull Eng Geol Environ, 2021; 80: 5575-87.

[29] Zhou Zhong, Fu Helin, Liu Baochen, et al. Experimental study on artificial rainfall simulation of soil-rock mi xture slope[J]. Rock and Soil Mechanics, 2007, 28(7): 1391-1396. (in Chinese)

[30] Li Rongjian, Bai Weishi, Wang Zhijun, et al. Research progress and key problems of rainfall slope test[J]. Sci ence and Technology Review, 2019, 37(14): 59-65.

[31] Yang Zongji, CAI Huan, Lei Xiao-Qin, et al. Soil and Rock Mechanics, 2019, 40(05): 1869-1880. (in Chines e)

[32] HORTON R E. The role of infiltration in the hydrologic cycle[J]. Transactions American Geophysical Union, 1933, 14(1): 446460.

[33] CUI Y F, ZHOU X J, GUO C X. Experimental study on the moving characteristics of fine grains in wide gr ading unconsolidated soil under heavy rainfall[J]. Journal of Mountain Science, 2017, 14(3): 417—431.

[34] Zhou Xiaojun. Research on strength, permeability characteristics and meso-structure of wide-graded gravel soil [D]. Chengdu: Chengdu Institute of Mountain Hazards and Environment, Ministry of Water Resources, Chines e Academy of Sciences, 2012. (in Chinese)

[35] LEI X Q, YANG Z J, HE S M, et al. Hydro-mechanical analysis of rainfall-induced fines migration process within unsaturated soils[J]. Journal of Mountain Science, 2017, 14(12): 2603-2619.

FUNDING

Youth Foundation of National Natural Science Foundation of China, Research on Velocity Regulation Mechanism and Application of Energy Dissipator in Debris Flow Drainage Channel (41807252)

ABOUT THE AUTHOR

Yicheng LIU was born in Shangrao, Jiangxi Province, China in 2001. He received his bachelor's degree from Nanchang Institute of Engineering and his postgraduate degree from the Department of Geology, Northwest University. His main research interest is geological disaster prevention and control.

E-mail: 13479370959@163.com

Fei WANG was born in Xi 'an, Shaanxi Province in 1989. He received his bachelor's degree from Sichuan University and his master's degree from Chengdu Institute of Mountain Hazards and Environment, Ministry of Water Resources, Chinese Academy of Sciences. His main research interests are debris flow mechanism and mountain disaster prevention.

E-mail: wf@nwu.edu.cn

Jiading WANG graduated from the Department of Applied Geophysics, Chang 'an University in July 1983 with a Bachelor's degree in engineering. From September 1983 to July 1986, he studied for a master's degree in seismic engineering at Lanzhou Institute of Seismology, State Seismological Administration, and later engaged in scientific research. He has been working at Northwestern University since August 1994. Among them, from September 1996 to June 1999, he studied for a doctoral degree in Geological Engineering in Chengdu University of Technology and obtained the Doctor of Engineering degree. From May 1999 to April 2001, he worked as a research fellow at the Geological Engineering Postdoctoral mobile Station of Jilin University. He has been abroad for further study and high visits. He was promoted to professor in 1999 and doctoral supervisor in 2001. In 2014, he was awarded the second-level professor by Shaanxi Province.

E-mail:wangjd@nwu.edu.cn

Yun LI was born in Xi 'an, Shaanxi Province in 1989. He graduated from Chengdu Institute of Mountain Hazards and Environment, Ministry of Water Resources, Chinese Academy of Sciences. He is currently working as a senior engineer in China Railway Changjiang Traffic Design Group Co., LTD., mainly engaged in route geological survey and highway subgrade design.

E-mail: liyuncdut@163.com